

Committee 5
Non-linear Structures in Natural Science and Economics

Draft – January 1, 2000
For Conference Distribution Only



The Methods of Non-linear Dynamics in the Analysis of Heart Rate Variability

Jaan Kalda
Senior Research Fellow
Institute of Cybernetics
Tallinn Technical University
Tallinn, Estonia

The Twenty-second International Conference on the Unity of the Sciences
Seoul, Korea February 9-13, 2000

INTRODUCTION

Certain cardiac arrhythmias can lead to a sudden cardiac death. Therefore, an important problem of cardiology is to define the prognostic significance of the heart arrhythmias. For this purpose both invasive and non-invasive methods are used. The non-invasive methods are preferable, because they pose less danger to the patients and are less expensive. The most wide-spread non-invasive methods are high-resolution electrocardiogram (ECG) for the detection of late potentials and Holter-monitoring. In the case of Holter-monitoring, ECG is monitored during 24 hours under the normal daily activities of the patient by portable light-weight recording apparatus. Both methods are widely used in clinical practice.

In addition to these methods, the analysis of the heart rate variability (HRV) has become an important tool in medical practice. This analysis is based on the sequences of the so-called normal-to-normal (NN) intervals t_{NN} . In a continuous ECG record (see Fig. 1), each complex corresponding to a single heart

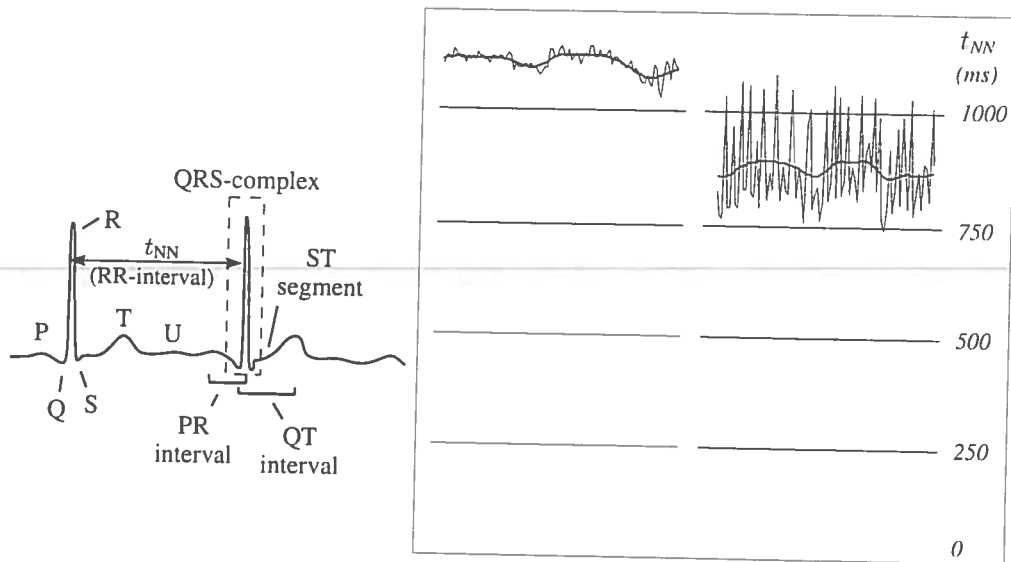


Figure 1: Left image: normal ECG recording. Image at right: t_{NN} sequences of low- and high variability. rhythm is detected. Usually the heart rhythm is defined via the distance between two R-pikes of the ECG-record and t_{NN} is measured as the interval between two adjacent *non-arrhythmic* QRS complexes (see Fig. 1). The current widespread use of the HRV-based characteristics is a result of the extensive studies during

the last two decades.

The clinical relevance of HRV was first noted in 1965 by Hon and Lee [1]. An increased risk of post-infarction mortality was associated with the reduced HRV by Wolf et al. in 1977 [2]. Wider attention to the problem has been attained in the early 1980s, when Akselrod et al. introduced the spectral methods for the HRV analysis [3]. The spectral characteristics are generally referred to as “frequency-domain characteristics” and are opposed to the “time domain methods”, which are derived directly from the t_{NN} -sequence. In the late 1980s, the clinical importance of HRV became generally recognized. Several studies confirmed that HRV was a strong and independent predictor of mortality following an acute myocardial infarction [4–6].

Currently, the following parameters are used in medical practice: the mean NN interval; the difference between night and day heart rate; longest and shortest NN intervals; the standard deviation of the NN interval (SDNN, typically calculated over 24-hour period); the standard deviation of locally (usually 5 min) averaged NN intervals (SDANN); the mean of the 5-minute standard deviation of the NN interval (averaged over 24 h; SDNN index); the square root of the mean squared differences of successive NN intervals (RMSSD), the percentage of interval differences of successive NN intervals greater than 50 ms (pNN50), the spectral power of high- and low-frequency fluctuations in NN-sequences.

It is widely accepted that the heart rhythm generation in the complex formed by sinus-node and atrio-ventricular node can be well described by nonlinear dynamical models [7,8]. This understanding has led to the idea that the dynamical characteristics from the theory of non-linear dynamics could be used for the diagnostic purposes. The early studies by Babloyantz et al. [9] gave rise to extensive studies in 1990s [10–13].

Currently, the main attention of the researchers is concentrated on the scale-invariant aspects of the HRV [14–20]. A non-complete list of the parameters which have been considered is as follows:

- the scaling properties of the Fourier spectra (the $1/f$ -law) [14];
- correlation dimension, Lyapunov exponents, and Kolmogorov entropy [9];

- distribution of points in three-dimensional (3D) phase space, particularly described by distribution of “words”, and Shannon, renormalized, and Renyi entropies [11];
- approximate entropy as the measure for the complexity of ECG sequence [12];
- distribution of points in phase spaces of higher dimensionality, particularly described by density distribution [20];
- the Hurst exponent H [15];
- long-range anticorrelation in time series [16];
- wavelet spectra [19];
- multifractal distribution of the Hurst exponent [17];
- multiscaling Zipf’s-law exponents [20]

It may seem quite strange that despite of the extensive studies and (as it has been claimed) good prognostic results, none of the above mentioned “nonlinear” characteristics has been found its application to the HRV analysis in medical practice. The researchers have been paid main attention to the study of the patients with increased risk of sudden cardiac death. The best prognostic significance has been obtained with the scale-invariant methods (based on Hurst exponent and wavelet spectra). However, no systematic study has been conducted to investigate large patient populations using these methods. The lack of this kind of studies seems to be the main reason, why there has been no major breakthrough by their application to the HRV analysis in medical practice.

In the present paper we follow two goals. The first one is to clarify the possibilities of using the characteristics based on the analysis of phase-space in medical practice for diagnostic purposes. The second one is to study the scale-invariant features of the non-stationary time-series generated by the heart rate.

HEART RATE GENERATION, ECG, AND DATA ACQUISITION

The quasi-periodic contraction of cardiac muscle is governed by the electrical signal, which is generated by the sino-atrial (SA) node — a set of electrically active cells in a small area of the right atrium. The signal spreads through the atrial muscle leading to its contraction. It also spreads into a set of specialized cells - the atrio-ventricular (AV) node. Further the signal spreads via the His-Purkinje bundle (which is a fractal-like set of electrically conductive fibers) to the myocardial cells causing their contraction. ECG is measured as the electrical potential between different points at the body surface. The activity of the SA node by itself is not reflected on the ECG. The electrical activation of the atrial cells leads to the appearance of the P-wave of the ECG. Q, R, S and T waves are caused by the electrical activity of the ventricular muscle. The heart rate is generally measured as the RR-interval t_{RR} — the time-lag between two subsequent R-pikes (R-pike itself corresponds to the ventricular contraction). For the HRV analysis, only the normal heart activity is taken into account. All the QRS-complexes are labelled as normal or arrhythmic. Note that even for healthy patients, some heartbeats can be arrhythmic. Normal-to-normal interval t_{NN} is defined as the value of t_{RR} for such heartbeats, which have both starting and ending R-pikes labelled as normal.

Typically, HRV analysis is based on the 24-hour recordings of the *Holter-monitoring*. Shorter ECG recordings can be used for this purpose, as well; however, in that case it is impossible to observe the long-scale variations and compare the sleep-awake differences in the heart rhythm. Portable apparatus stores the ECG data as the time-dependent voltage $U(t)$ either on a tape or on a PC flash card; the sampling rate is 125 Hz or higher. The data are later analyzed by computer software. Typical commercial software allows visualization of the ECG recording, automated or semi-automated recognition of arrhythmias and artifacts, and the calculation of the standard “linear” characteristics of the HRV. Most often, a research devoted to the methods of non-linear dynamics is based on plain sequences of NN-intervals, and disregards the details of the continuous ECG recordings.

The experimental data serving as the bases of this research were recorded at the Tallinn Nõmme Hos-

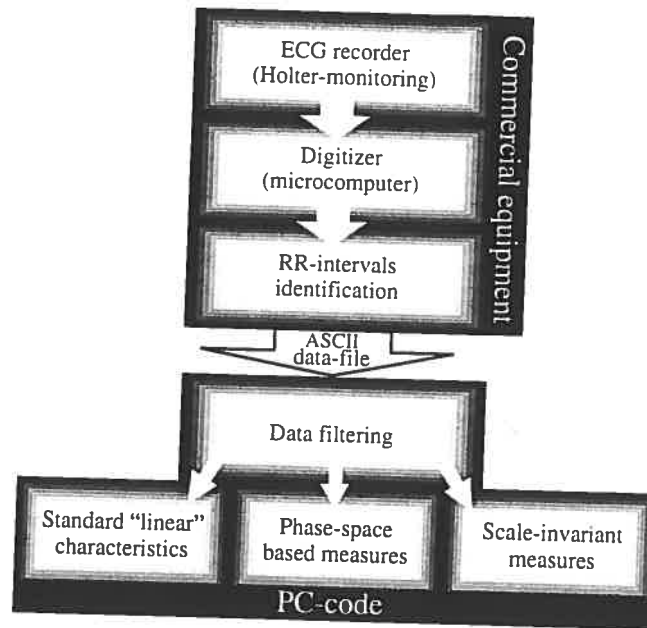


Figure 2: The analysis of the heart rate variability: the scheme of data acquisition and analysis.

pital; the scheme of data acquisition is presented on Fig. 2. The recordings of the ambulatory Holter-monitoring of healthy children (group of 12 subjects, mean age 11.5 ± 3.3 years) and children with clinically documented sinus node disease (6 subjects, mean age 11.5 ± 1.9 years) were used. There was also a heterogeneous group of 12 subjects with miscellaneous diagnosis. The sampling rate of the ECG was 125Hz, corresponding to the resolving power of 8ms.

PHASE-SPACE METHODS

Nonlinear dynamical models of the heart rate generation consider SA node and AV node as nonlinear coupled oscillators [7,8]. The model has been proven to be viable and predicts several experimentally observed phenomena, such as Wenckebach and Mobitz type II arrhythmias and bistable behavior [8]. This deterministic non-linear model predicts that the phase trajectories of a healthy heart lie on an attractor of the coupled system of oscillators. Consequently, one should be able to observe well-defined patterns on the Poincarè sections of the phase-space. Note that in the case of physiological data, there is no information,

what might be the canonical variables. Therefore, the phase trajectory is reconstructed in time-delay coordinates $U(t), U(t + \tau), \dots, U[t + (D - 1)\tau]$ [or $t_{NN}(n), t(n + 1), \dots, t(n + D - 1)$]. Here D is the so called embedding dimensionality, i.e. the dimensionality of the reconstructed phase-space. It is expected that the real phase trajectory is mapped to the reconstructed trajectory by a smooth transform.

Such a behavior has been observed indeed in several experimental studies. Particularly, the correlation dimension of the continuous ECG recording (i.e. the recorded voltage as a function of time) has been reported to be between 3.6 and 5.2; the correlation dimension of the plain t_{NN} -sequences of healthy patients has been found to be 5.9 ± 0.4 [20]. A wide-spread conclusion has been that the dynamics of the heart of healthy persons is less regular than that of persons with severe cardiac pathologies. Correspondingly, the correlation dimension is often thought to be a measure for the healthiness of the heart.

The correlation dimension of a data sequence can be calculated according to the Grassberger-Procaccia algorithm [21]. In a reconstructed phase space of dimensionality D , the correlation integral $C = \sum_{i,j} \theta(r - |r_i - r_j|)$ is calculated as a function of the radius r ; it is expected to behave as a power-law $C \propto r^{\nu(D)}$. Here r_i denotes the D -dimensional radius-vector of the i -th data-point, and $\theta(r)$ stands for the Heaviside function. The correlation dimension d_c is found as the limit of ν at large values of D (in fact, it is expected that for $D > d_c$, the exponent ν is independent of D , and in that case $\nu = d_c$).

The reliability of the calculation of the correlation dimension has been sometimes questioned, c.f. [13]. This is because the heart is not an isolated system. Instead, the rhythm generated by sinoatrial node is essentially affected by non-deterministic inputs from parasympathetic and sympathetic branches of nervous system. This leads to a more complex behavior of the heart rhythm. There are diverse physiological origins for those inputs, some of which lead to quasi-periodic signals. Thus, respiration gives rise to the signal of typical period of 4s; the effect is most pronounced when the patient is at rest, and is stronger for young persons. In addition, there is a signal caused by blood-pressure oscillations, which has a typical period of 10s (there is no unique view on the origin of the blood-pressure oscillations; sometimes it is believed to be a

resonance phenomenon caused by a time-delay in the feed-back loop of the blood pressure control system). Therefore, the deterministic signal formed inside the heart is modulated by inputs arriving from the autonomic nervous system. The inputs may be quasi-periodic, but are still uncorrelated with the deterministic signal. This “random” component distorts the attractor trajectories (and their projections to the time delay maps).

Another source of difficulties is the length of the data sequences, which may be inadequate for reliable calculation of high values of the correlation dimension. This aspect has been studied via the analysis of surrogate data. Thus, in [13] it has been reported that in the case of low dimensionality ($d_c \lesssim 3$), the surrogate data (i.e. the real experimental data shuffled in a random way) yield clearly higher values of d_c than the original data. Therefore, one can be sure that the observed variations of the signal are distinct from noise. In the case of $d_c \gtrsim 4$, the distinction between the surrogate data and the original data is less clear.

Note that the surrogate data analysis does not answer the question, how well does the signal correspond to a nonlinear dynamical model. Instead, it addresses the question, is the signal distinct from noise or not. In what follows we argue that typically, the low values of d_c do not evidence a low-dimensional dynamical chaos inside the heart, because the signals arriving outside the heart lead to a significant distortion of the phase-space trajectories. Particularly, the modulation of the heart rhythm by signals generated by respiration has a considerable effect on the observed values of the scaling exponent d_c . There is also a simple explanation to the fact that the healthy heart behaves more randomly than sick heart: it is more responsive to the whole spectrum of signals arriving from the autonomous nervous system. To sum up, we are not claiming that the calculation of d_c is meaningless; however, in most cases, the term “correlation dimension” does not reflect the real physical meaning of this scaling exponent.

We approached the problem of the nonlinear dynamic nature of the heart rate dynamics in the simplest possible way: we studied visually the two-dimensional cross-sections of the phase space for $D = 3$ and $D = 4$. This is almost trivial approach; however, in earlier studies it has not been exploited in a systematic

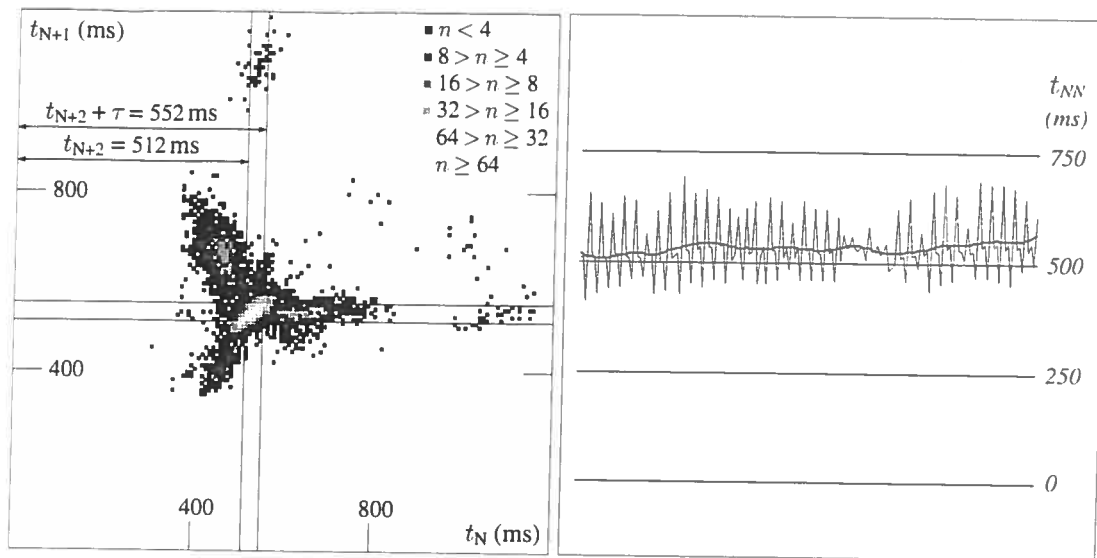


Figure 3: A cross-section of the 3-dimensional phase space; around the central cloud of points, three major satellite-clouds can be seen; these satellite-clouds correspond to the sequence of interbeat intervals, shown on the right-hand plot. The observed oscillations with period 4 can be attributed to the modulation of the heart rate by respirations.

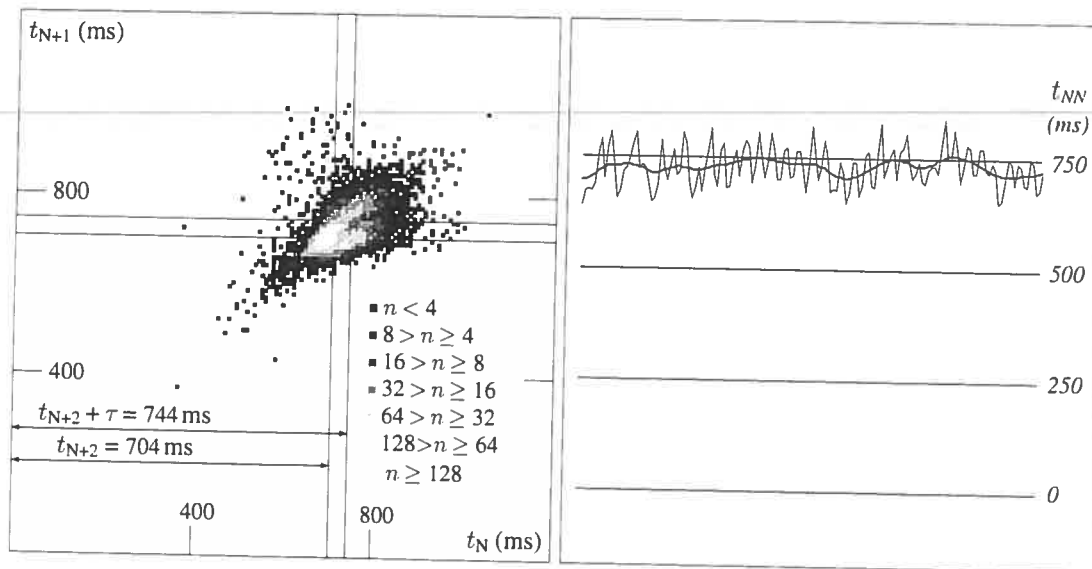


Figure 4: The same as on Figure 3. There are no satellite clouds; however, one can distinguish two branches of the central cloud, which are again caused by the respiratory modulation.

way (the cross-sections are not to be confused with the simple projections of the phase-space to plane, which can be found for $D = 3$, c.f. [9]). The lack of such kind of studies can be probably attributed to the high dimensionality of the expected attractor and difficulties in visualizing the high-dimensional patterns.

If a patient with a serious heart diseases has $d_c < 4$, one should be able to observe a “patterning” of points on the cross-sections of the phase-space. The phase-space was reconstructed using t_{NN} -sequences; it was divided into boxes of equal size ($8\text{ms} \times 8\text{ms} \times \tau$ for $D = 3$ and $8\text{ms} \times 8\text{ms} \times \tau \times \tau'$ for $D = 4$). Further, the number of points per each box was counted. The results were presented on a two-dimensional plot; the position of the cross-section and the box heights τ and τ' were selectable parameters, see Fig. 3 and 4 (different grey levels correspond to the different number of points per box).

For a major part of the patients, the points were randomly distributed over the cross-section forming a “cloud” of an irregular shape (*case A*) and with almost no patterning of points. For some patients, there were smaller “clouds” surrounding the central one (*case B*). It might seem tempting to interpret these “satellite-clouds” as an indication of a decreased dynamical chaos with a lowered correlation dimension. However, these “satellite-clouds” were much less populated than the central one, so that the standard quantitative methods of the phase-space analysis were unable to make a reliable discrimination between the two cases.

We found that the most sensible method of discriminating between the cases A and B was based on the fluctuation function $F(n) = \langle |t_{NN}(n+m) - t_{NN}(m)| \rangle_m$; angular brackets denote averaging over the values of m . For the patients with “satellite-clouds” in phase space, the function $F(n)$ had significant oscillations at small values of n (Fig. 5). Owing to this, the amplitudes of the short-scale components of discrete Fourier transform were chosen to characterize the patterning in phase space. In order to minimize the influence of the long-scale components, the transform was applied to the function $G(n) = F(n) - \tilde{F}(n)$. Here $\tilde{F}(n)$ denotes the smoothed (averaged and interpolated) fluctuation function $F(n)$. In order to locate the periods responsible for the formation of the “satellite-clouds” in time, the 24-hour recording was divided into 1-hour sub-intervals and the calculations were performed for all those intervals. The distribution of the

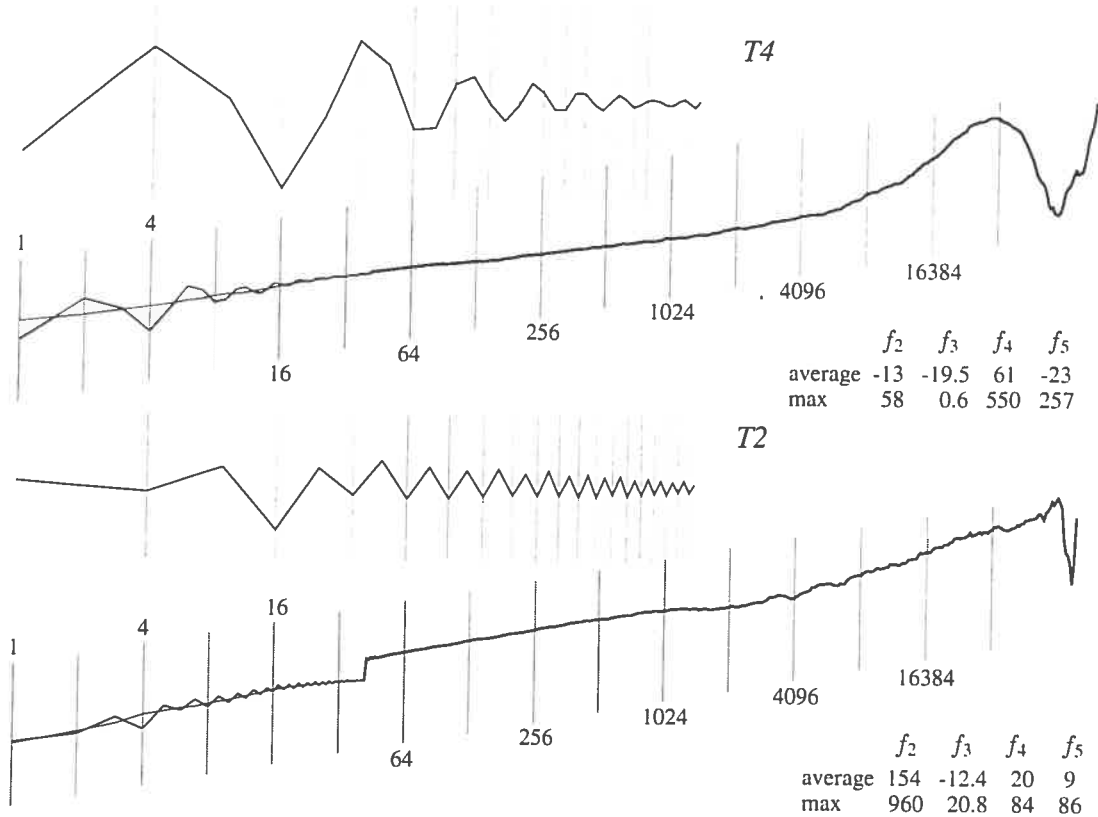


Figure 5: Fluctuation functions for patients T2 and T4. The left-hand part of the graph is characterized by periodic oscillations, the period being equal to 2 and 4, respectively. The jump at the beat number 36 is due to different methods of treating the sequences containing non-qualified (artifactual or arrhythmic) beats above and below this delay value.

Fourier amplitudes over the time intervals turned out to be very inhomogeneous; typically, a clear peak has been achieved between 22.00 and 2.00.

In order to analyze visually the heart rate dynamics, the graphs plotting t_{NN} versus the beat number n were used. The visual analysis of the periods corresponding to the largest Fourier amplitudes revealed that the common characteristic feature of them is an highly periodic variation of the NN-intervals; the oscillation period τ (measured in beat numbers) was the same as in the case of the fluctuation function $F(n)$, and changed from $\tau = 2$ to $\tau = 5$ (Fig. 6).

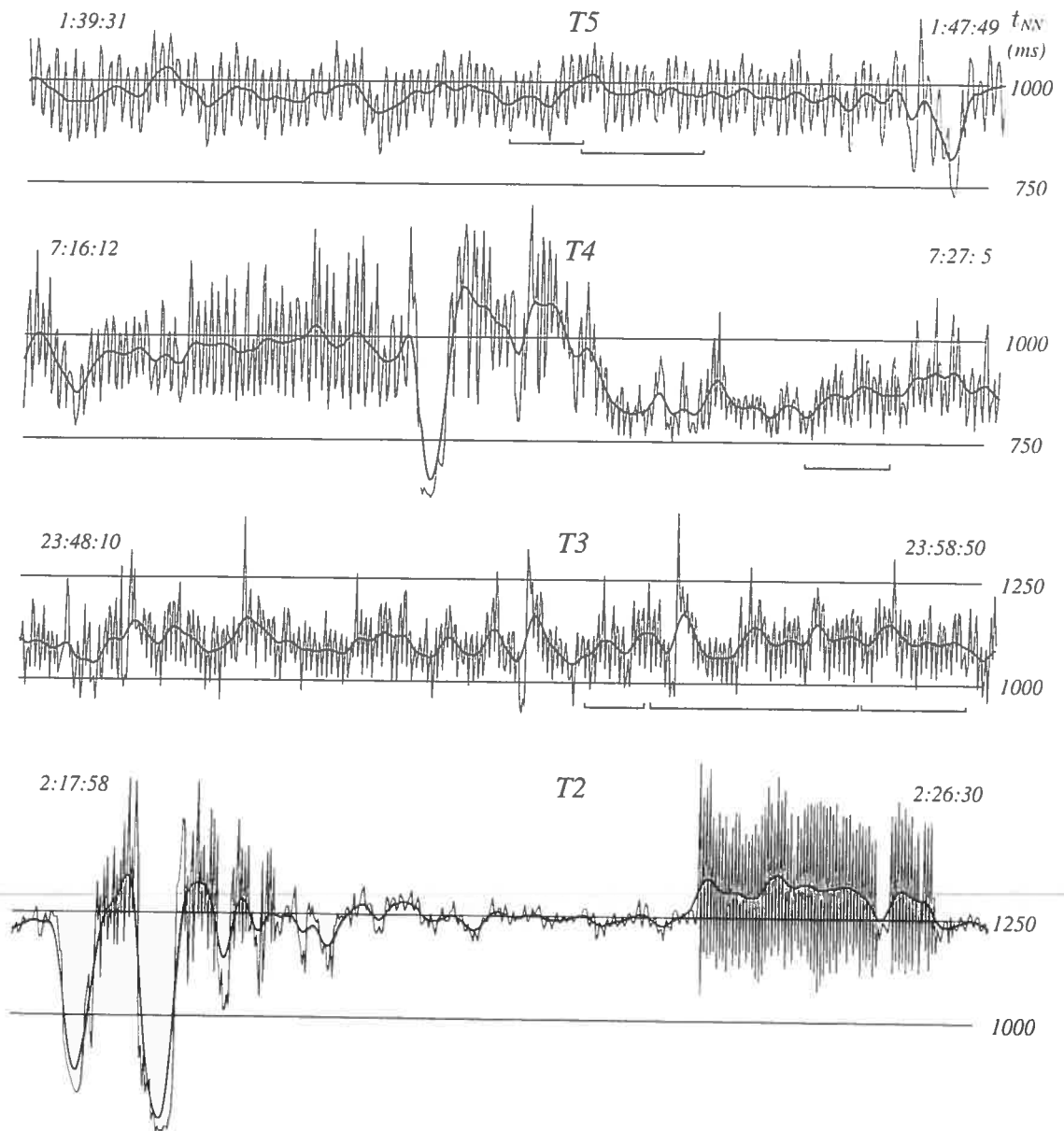


Figure 6: The duration of NN-intervals plotted versus the beat number. For patients $T3$ – $T5$, the horizontal lines indicate the periods where the correlation between the heart rate and its respiratory modulation are maintained. For patient $T2$, the highly periodic behavior at the right-hand part of the plot can be interpreted as a result of the low-dimensional chaos in the complex responsible for the heart rate generation.

The high-frequency ($f \approx 0.5\text{Hz}$) component of the HRV is known to be caused by respiration. Thus, it is natural to assume that these periodic oscillations of the time series t_{NN} , which are seen on Fig. 6, are due to the respiratory modulation; the period is defined by the ratio of the heart rate and respiratory frequencies. This conclusion is confirmed by the observation that after a certain time, the coherence between the heart rhythm and the periodic modulation is lost (the only exception is the patient with $\tau = 2$; here the periodic behavior is likely to be caused by a true non-linear dynamics of the heart).

Therefore, we can claim that in the case of healthy children and children with SND, there is no ground to speak about the low-dimensional chaos of the heart rhythm; the “patterning” in phase space (if present) gives evidence that during certain time-periods (typically, when the patient is at rest), the heart rhythm is significantly affected by respiration, and the ratio of the local mean heart rate to the respiration frequency is almost constant. This claim is likely to be valid for a significantly wider range of patients; however, in order to increase the reliability of the conclusion, the statistical basis of the analysis is to be extended.

If we accept that the phase-space trajectories do not reflect the non-linear dynamical nature of the heart dynamics, then we have to admit that d_c , calculated according to the Grassberger-Procaccia algorithm [21], is nothing more than just a scaling exponent. This scaling exponent has been found to be capable of distinguishing the patients with heart failure from the healthy patients. Then, perhaps there are some other characteristics describing the distribution of points in phase space, which can be also used for diagnostic and/or prognostic purposes? To address this question, the density distribution of points in the phase space has been studied as follows. The phase space has been divided into hypercubes of equal size — 2% of the average value of the NN-interval. The number of points K in each hypercube has been calculated, and for each K , the number of hypercubes $M(K)$ containing more than K points has been counted. In order to make the result independent of the length of the data-sequence, the number K was reduced to the total number of points in the phase-space: $k = K/K_{\text{tot}}$. The function $M(k)$ can be conveniently plotted on the logarithmic graph. Comparing the graphs of different patients revealed that the most representative single

characteristic of the graph (i.e. the number, which is the most sensitive with respect to the diagnosis of the patient) is the maximal value of $k - k_{\max}$. The patients with sinus node disease had significantly lower values of k_{\max} than the other patients. The difference was most explicit in the case of eight-dimensional phase space (Fig. 7). On the figure, LPDD8PS means “the logarithm of the peak density distribution of points in eight-dimensional phase space”, and is equal to $\log k_{\max}$. It should be noted that the highest density of points was always observed in that region of the phase space, where all the coordinates were equal to each other. Thus, only the low-variability periods with almost equal subsequent NN-intervals contribute to LPDD8PS. In addition, the patients with very high values of LPDD8PS had long periods of almost constant heart rate. Such a behavior is not characterized by the standard “linear” characteristics of HRV. However, in some extent, the values of pNN50 are affected: the correlation between these two characteristics is observable (Fig. 7), but not very strong. Therefore, LPDD8PS can potentially contain independent diagnostically useful information and deserves further analysis.

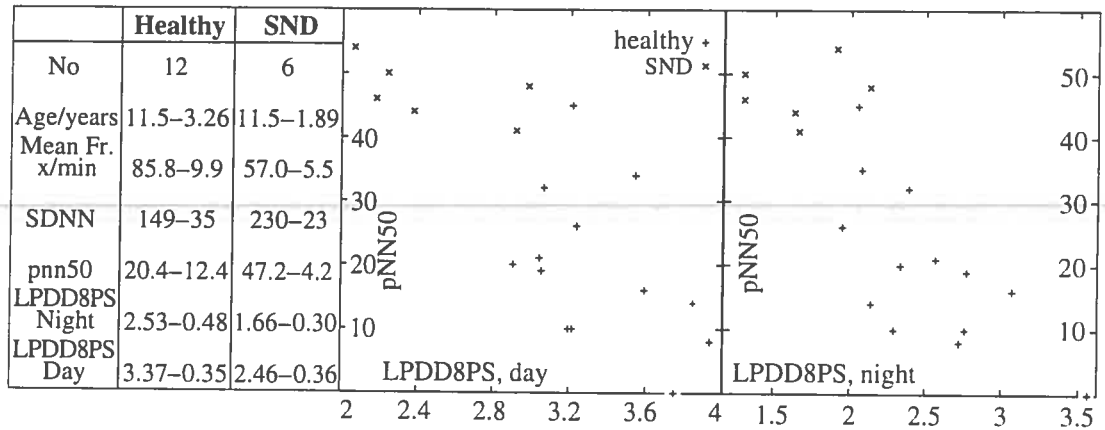


Figure 7: Healthy subjects (denoted by “+”) and patients with sinus node disease (denoted by “x”): statistical data and distribution on the plane defined by pNN50 and LPDD8PS.

SCALE-INDEPENDENT MEASURES.

Recent studies have shown that scale-invariant characteristics can be successfully applied to the analysis of the heart rate variability [16–18]. However, this conclusion has been disputed, and certain scale-dependent measures (particularly, the amplitude of the wavelet spectra at specific time-scale) have been claimed to provide better results [19]. As a response, it has been argued that the scale-dependent methods may reflect characteristics specific to the subject and/or to the method of analysis and therefore require special caution in applications; certain heart disorders affect the heart rate variability at a specific scale or range of scales; owing to this circumstance, at the properly chosen time-scale, scale-dependent measures may provide a useful information. Meanwhile, the scale-independent methods are more universal, subject-independent, and reflect directly the dynamics of the underlying system [18].

The simplest relevant scale-independent measure is the Hurst exponent H , which has been introduced to describe statistically self-affine random functions $f(r)$ of one or more variables [22]. Such a function is referred to as *fractional Brownian function* and satisfies the scaling law

$$\langle [f(r_1) - f(r_2)]^2 \rangle \propto |r_1 - r_2|^{2H}.$$

Note that $H = 1/2$ is a special case of ordinary Brownian function — the increments of the function are delta-correlated, and $f(r)$ can be thought to be the displacement of a Brownian particle as a function of time r . Therefore, in the case of $H < 1/2$, there is a negative long-range correlation between the increments of the function. Analogously, $H > 1/2$ corresponds to a positive correlation.

Many phenomena in nature exhibit this kind of scale-invariance, and lead to fractional Brownian time-series [22]. The same is true for heart rate variability: after filtering out short-scale components with $\tau < 30$ s (corresponding to the respiratory rhythm, to the blood-pressure oscillations, and to the pathological Cheyne-Stokes respiration), the fluctuation function $F(n)$ revealed a good scaling behavior $F(n) \propto n^H$ [16]. While for healthy patients, the increments of the heart rhythm were significantly anticorrelated re-

sulting in $H < 1/2$, the heart rhythm of the patients with dilated cardiomyopathy was essentially Brownian with $H \approx 1/2$.

It has been pointed out that the NN-sequences of healthy subjects consist of intertwined high- and low-variability periods [10]. This conclusion can be easily verified by simple visual observation of the NN-sequences, see Fig. 8. Typically, such an intermittent behavior can be adequately described by multifractal formalism. Note that multifractality is a more general scale-invariant behavior than a plain fractality. Therefore, unless there is a special mechanism leading to a plain fractality, one can expect that a scale-invariant phenomenon is multifractal. Recent results [17] indicate that for healthy patients, the local values of the Hurst exponent $H(n)$ (defined via the scaling law $\langle |t_{NN}(n+m) - t_{NN}(m)| \rangle \propto n^H$) reveal, indeed, a multifractal distribution, which can be described by the spectrum of exponents $f(H)$.

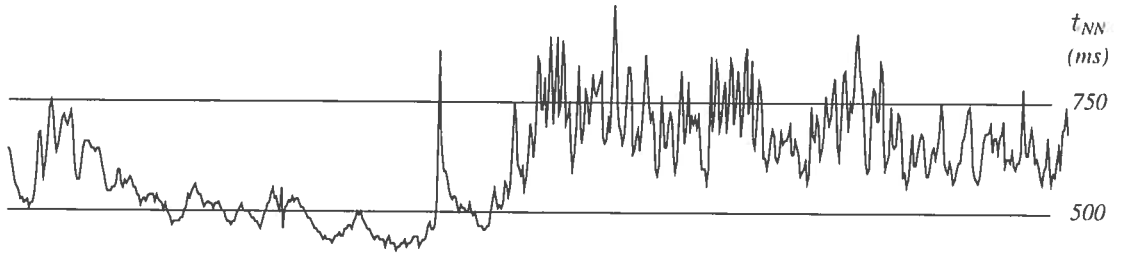


Figure 8: For healthy patients, the high- and low-variability periods of the heart rhythm are intertwined.

An alternative approach to the multiscaling analysis of NN-sequences is based on the Zipf's law. Originally, the law has been formulated by George Kingsley Zipf for the frequency of words in natural languages. For a given language (e.g. english), the frequency (the number of occurrences divided by the total number of words) of each word is calculated on the bases of a large set of texts. The ranks are determined by arranging the words according to their frequency f : the most frequent word obtains rank $r = 1$, the second frequent — $r = 2$ etc. It turns out that for a wide range of ranks (starting with $r = 1$), there is a power law $p(r) \propto r^{-\alpha}$, where $\alpha \approx 1$. This law is universal, it holds for all the natural languages and for a wide variety of texts [23]. Furthermore, similar scaling laws describe the rank-distribution of many other classes of objects, as

well. Thus, when cities are arranged according to their population s , the population of a city $s \propto r^{-\alpha}$, with $\alpha \approx 1$ [23]. Another example is the income-rank relationship for companies; here we have again $\alpha \approx 1$ [23]. In the most general form, the law can be formulated as $p \propto (r + r_0)^{-\alpha}$, and α is not necessarily close to unity [24]. The more general form of the law can be applied to the distribution of scientists according to their citation index, to the distribution of internet sites according to the number of visitors etc.

Here we apply the Zipf's law to the distribution of low heart rate variability periods according to their length. We define the local heart rate variability as the deviation of the heart rate from the local average,

$$\delta(n) = [t_{NN}(n) - \langle t_{nn}(n) \rangle] / \langle t_{nn}(n) \rangle;$$

the local average is calculated using a narrow (≈ 5 -second-wide) Gaussian weight-function. The low-variability regions are defined as consecutive sequences of intervals with $|\delta(n)| < \delta_0$; the length l of such a region is measured as the number of beats in the sequence. Further, all the low-variability regions are

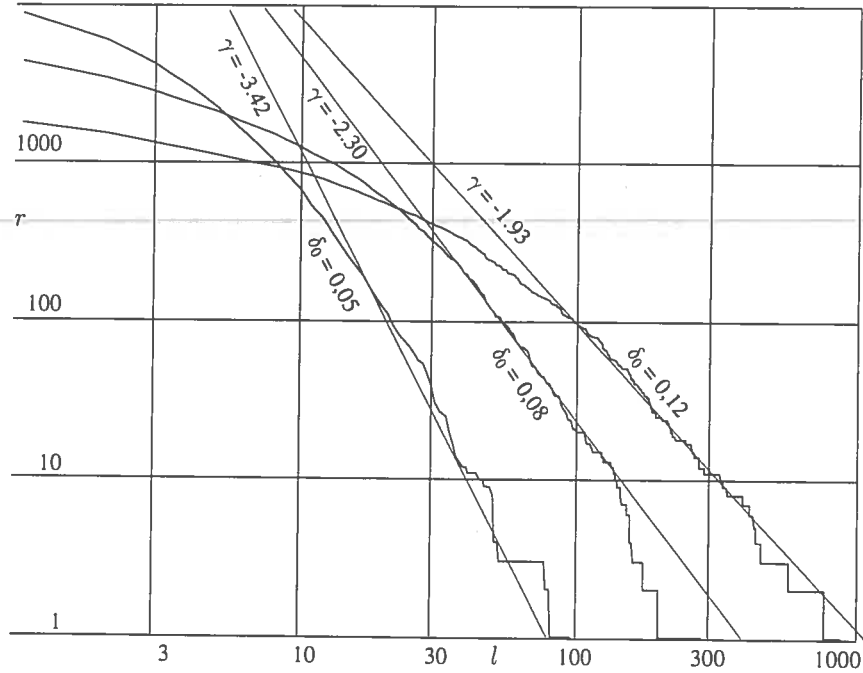


Figure 9: Multi-scaling behavior: the rank of low-variability intervals is plotted against the length of the intervals. The scaling exponent γ depends on the threshold value δ_0 .

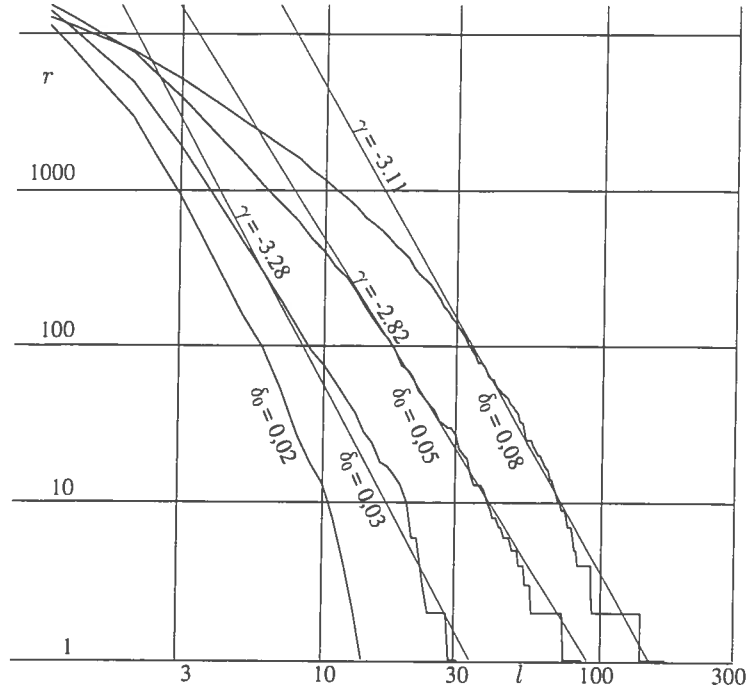


Figure 10: Mono-scaling behavior: the rank of low-variability intervals is plotted against the length of the intervals. The scaling exponent γ depends on the threshold value δ_0 .

numbered (to identify them later), and arranged according to their length; regions of equal length are ordered randomly. In such a way, the longest observed region obtains rank $r = 1$, second longest — $r = 2$, etc. It turns out that for healthy children, the length-rank relationship reveals multiscaling properties, i.e. within a wide range of scales, $l \propto r^\alpha$, where the scaling exponent is a (non-constant) function of the threshold level, $\alpha = \alpha(\delta_0)$; see Fig. 9. Meanwhile, for the patients with SND, there was no multiscaling, i.e. either the scaling exponent was independent of the value of δ_0 , or the inertial range of scales was too low to make any meaningful calculations; see Fig. 10. It should be noted that the author is not aware of the earlier reports of Zipf's-law-like multiscaling behavior in nature.

One may ask, why did we analyze the distribution of low-variability periods, and not, for instance, the distribution of high-variability periods. There are two reasons for this. First, if we define the high-variability regions in a straightforward way as the consecutive sequences of intervals with $|\delta(n)| > \delta_0$, there would be

no scaling at all, because potentially long sequences are broken into small pieces by those heart beat intervals t_{NN} , which are, by accident, equal (or very close) to the local mean $\langle t_{NN}(n) \rangle$. Second, even if we define the high-variability periods in a more clever way, the distribution of low-variability periods would be still of greater physiological interest, because for a healthy heart, the low variability is typically caused by a high level of competing inputs arriving from the autonomous nervous system (i.e. by “stress” conditions).

Finally, we introduced the length l of the longest low-variability region for a fixed threshold level $\delta_0 = 0.05$ (LLLR) as a candidate for a single number characterizing the distribution of low-variability periods. Note that LLLR is highly correlated with the scaling exponent α at $\delta_0 = 0.05$. Indeed, the number (and hence the rank) of very short low-variability regions is almost patient-independent. Bearing this in mind, and assuming a perfect scaling over all the scales, the two above mentioned parameters are directly related to each other. Note that, for some patients, $\alpha(0.05)$ is not well defined due to a pure scaling behavior; meanwhile, LLLR can be always easily calculated.

It should be noted that LLLR and LPDD8PS are related to each other. High values of LLLR give rise to high values of LPDD8PS; the opposite is not always true. Indeed, all the points from a single low-variability region fall into a single cell of the phase-space. Similarly to LPDD8PS, LLLR yielded a good distinction between the two groups of patients. For the group of healthy subjects, $LLLR = 132 \pm 90$; the patients with SND resulted in $LLLR = 51 \pm 14$. According to the Student test, the two groups were distinct with the probability of $p = 0.9\%$. Further analysis of the clinical applicability of this parameter is encouraged by the fact that for some patients of the heterogeneous group, extremely high values — up to $LLLR=378$ — were achieved.

CONCLUSIONS

Human heart rate fluctuates in a complex and non-stationary manner. During last decades, a wide variety of methods have been suggested to analyze the time sequences of the heart beat intervals. The following

classification of the methods can be constructed.

1. “linear” methods — based on simple statistical measures and on the Fourier analysis. These are the only methods, which are widely used in clinical practice.
2. “nonlinear” methods:
 - (a) scale-invariant methods:
 - i. based on fractional Brownian functions and Hurst exponent (including multifractal analysis);
 - ii. based on Zipf’s law;
 - (b) scale-dependant methods:
 - i. based on phase-space analysis (including entropy-based measures and the correlation dimension);
 - ii. based on wavelet spectra at a specific time-scale.

Here we have argued that typically, the correlation dimension does not reflect the nonlinear dynamics of the heart. Instead, it should be treated as a scaling exponent characterizing the distribution of data points on time-delay maps; its value is greatly affected by the signals arriving into the heart from the autonomous nervous system, particularly by the ones due to respiration.

We have also shown that the distribution of the low-variability periods of an healthy heart is described by the multiscaling Zipf’s law. We have introduced two new measures of HRV — LPDD8PS and LLLR. However, in order to achieve a real clinical application of them, further studies on wider experimental basis are needed.

ACKNOWLEDGMENTS

The author is very grateful to his student Maksim Säkki for performing the numerical analysis, and to Meelis Vainu and Mari Laan for providing the Holter-monitoring data, clinical diagnosis and consultation. This study has been partially supported by the Estonian Science Foundation grant No 3740.

REFERENCES

1. Hon E.H., Lee S.T., *Electronic evaluations of the fetal heart rate patterns preceding fetal death, further observations.* Am. J. Obstet. Gynec. **87**, 814–826 (1965).
2. Wolf M.M., Varigos G.A., Hunt D., Sloman J.G. *Sinus arrhythmia in acute myocardial infarction.* Med. J. Australia **2**, 52–53 (1978).
3. Akselrod S., Gordon D., Ubel F.A., Shannon D.C., Barger A.C., Cohen R.J. *Power spectrum analysis of heart rate fluctuation: a quantitative probe of beat to beat cardiovascular control.* Science **213**, 220–222 (1981).
4. Kleiger R.E., Miller J.P., Bigger J.T., Moss A.J., and the Multi-center Post-Infarction Research Group. *Decreased heart rate variability and its association with increased mortality after acute myocardial infarction.* Am. J. Cardiol. **59**, 256–262 (1987).
5. Malik M., Farrell T., Cripps T., Camm A.J. *Heart rate variability in relation to prognosis after myocardial infarction: selection of optimal processing techniques.* Eur. Heart J. **10**, 1060–1074 (1989).
6. Bigger J.T., Fleiss J.L., Steinman R.C., Rolnitzky L.M., Kleiger R.E., Rottman J.N. *Frequency domain measures of heart period variability and mortality after myocardial infarction.* Circulation **85**, 164–171 (1992).

7. West B.J., Goldberger A.L., Rooner G. and Bhargava V. *Nonlinear Dynamics of the Heartbeat. 1. The AV Junction: Passive Conduct on Active Oscillator*. *Physica D* **17**, 198 – 206 (1985).
8. Engelbrecht, J., Kongas, O. *Driven oscillators in modelling of heart dynamics*. *Applicable Anal.* **57**, 119–144 (1995).
9. Babloyantz A., Destexhe A. *Is the normal heart a periodic oscillator?* *Biol. Cybern.* **58**, 203–211 (1988).
10. Poon C.S., Merrill C.K. *Decrease of cardiac chaos in congestive heart failure*. *Nature* **389**, 492–495 (1997).
11. Voss A., Kurths, J., Kleiner, H.J., Witt, A., Wessel, N., Saparin, P., Osterziel, K.J., Schurath, R., and Dietz, R. *The application of methods of non-linear dynamics for the improved and predictive recognition of patients threatened by sudden cardiac death*. *Cardiovasc. Res.* **31**, 419–433 (1996).
12. Pincus, S., *Approximate entropy (ApEn) as a complexity measure*. *Chaos* **5**, 110–117 (1995).
13. Govindan, R.B., Narayanan, K., and Gopinathan, M.S. *On the evidence of deterministic chaos in ECG: Surrogate and predictability analysis*. *Chaos* **8**, 495 – 502 (1998).

14. Kobayashi M., Musha T. *1/f fluctuation of heart beat period*. *IEEE Trans. Biomed. Eng.* **29**, 456–457 (1982).
15. Yamamoto Y., Hughson R.L. *Coarse-graining spectral analysis: new method for studying heart rate variability*. *J. Appl. Physiol.* **71**, 1143–1150 (1991).
16. Peng C.K., Mietus, J., Hausdorff, J.M., Havlin, S., Stanley, H.E., and Goldberger, A.L. *Long-range anticorrelations and non-Gaussian behavior of the heartbeat*. *Phys. Rev. Lett.* **70**, 1343–1347 (1993).
17. Ivanov, P.Ch., Rosenblum, M.G., Amaral, L.A.N., Struzik, Z., Havlin, S., Goldberger, A.L., and Stanley, H.E. *Multifractality in Human Heartbeat Dynamics*, *Nature* **399**, 461–465 (1999).

18. Amaral, L.A.N., Goldberger, A.L., Ivanov, P.Ch., and Stanley, H.E., *Scale-Independent Measures and Pathologic Cardiac Dynamics*. Phys. Rev. Lett. **81**, 2388–2391 (1998).
 19. Thurner, S. Feurstein, M.C., and Teich, M.C., *Multiresolution wavelet analysis of heartbeat intervals discriminates healthy patients from those with cardiac pathology*. Phys. Rev. Lett. **80** 1544–1547 (1998).
 20. Kalda, J., Vainu, M. and Säkki, M. *The methods of nonlinear dynamics in the analysis of heart rate variability for children*, Med. Biol. Eng. Comp. **37**, 69–72 (1999).
 21. Grassberger, P. and Procaccia, J., *Measuring the strangeness of a strange attractor*, Physca D, **9**, 189–(1983).
 22. Mandelbrot, B.B., and Van Ness, J.V. *Fractional Brownian motion, fractional noises and applications*, SIAM Rev. **10**, 422-434 (1968).
 23. Zipf, G.K. *Human Behavior and the Principle of Least Effort* (Cambridge, Addison-Wesley, 1949).
 24. Mandelbrot, B.B. *The Fractal Geometry of Nature* (Freeman, San Francisco, 1983).
-